

NWRI - UNPUBLISHED REPORT

ENGEL, P (1980)

ENGEL

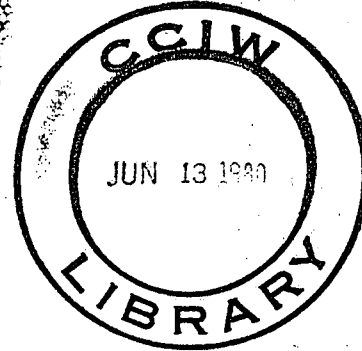


**Environment  
Canada**

**Environnement  
Canada**

**National  
Water  
Research  
Institute**

**Institut  
National de  
Recherche sur les  
Eaux**



**BED-LOAD DISCHARGE COEFFICIENT  
FOR MIGRATING DUNES**

by  
P. Engel

TD  
7  
E54  
1980a

**BED-LOAD DISCHARGE COEFFICIENT  
FOR MIGRATING DUNES**

by  
P. Engel

Environmental Hydraulics Section  
Hydraulics Research Division  
National Water Research Institute  
Canada Centre for Inland Waters  
April 1980

## TABLE OF CONTENTS

	<u>Page</u>
LIST OF TABLES	ii
LIST OF FIGURES	iii
SUMMARY	iv
MANAGEMENT PERSPECTIVE	vi
1.0 INTRODUCTION	1
2.0 LITERATURE REVIEW	2
3.0 ANALYTICAL CONSIDERATIONS	4
3.1 Background	4
3.2 Bed-Load Discharge Coefficient	4
3.3 Dimensional Analysis	5
4.0 EXPERIMENTAL EQUIPMENT AND PROCEDURE	7
5.0 DATA ANALYSIS	9
6.0 APPLICATION OF BED-LOAD COEFFICIENT	11
7.0 CONCLUSIONS	12
REFERENCES	13
ACKNOWLEDGEMENTS	15

## LIST OF TABLES

### Table Number

- 1 Experimental Data
- 2 Average Values of k
- 3 Bed-Load Discharge Coefficient K
- 4 Computed Bed Load Using  $K = K [\Delta/\Lambda, D_{50}/\Delta]$
- 5 Effect of Bed-Load Coefficient

## LIST OF FIGURES

### Figure Number

- 1 Definition Sketch
- 2 Dye Injection Apparatus
- 3a Dye Downstream of Re-attachment Point
- 3b Dye Upstream of Re-attachment Point
- 4 Variation of  $k$  with Froude No. when  $\Delta/\Lambda=0.02$
- 5 Variation of  $k$  with Froude No. when  $\Delta/\Lambda=0.033$
- 6 Variation of  $k$  with Froude No. when  $\Delta/\Lambda=0.05$
- 7 Variation of  $k$  with Froude Number when  $\Delta/\Lambda=0.07$
- 8 Effect of Sand Size on  $k$
- 9 Variation of  $k$  with Dune Steepness
- 10 Bed-Load Discharge Coefficient
- 11 Effect of Bed-Load Coefficient

## SUMMARY

Using dimensional analysis and experiments conducted in a rectangular flume, a bed-load discharge coefficient was developed. The coefficient was found to depend on bed-form steepness and relative sand grain size. The results showed that the bed-load coefficient is affected significantly by sand grain size only when the dunes are flat. When dunes are steep, the value of the bed-load coefficient is affected mainly by the dune steepness. Application of the bed-load coefficient resulted in some improvement of estimating bed load. However, it appears unlikely that estimates of bed load using the Hydrographic Method, even with the refinement of the bed-load coefficient, will be better than  $\pm 20$  percent of the true value.

## RÉSUMÉ

À partir d'analyses et expériences dimensionnelles effectuées dans une auge rectangulaire, on a élaboré un coefficient de débit charrié. On a constaté que le coefficient dépendait de la pente du fond et de la grosseur relative des grains de sable. D'après les résultats, le coefficient de débit charrié ne subit une modification importante sous l'influence de la grosseur des grains de sable qu'en présence de dunes planes. Quand les dunes sont abruptes, la valeur du coefficient de charriage de fond est modifiée surtout sous l'influence de la pente de la dune. Le recours au coefficient de charriage de fond a permis d'améliorer un peu l'évaluation du charriage de fond. Toutefois, en dépit du perfectionnement que constitue le coefficient de charriage de fond, il n'est guère probable que l'évaluation du charriage de fond, selon la méthode hydrographique, permette d'obtenir des résultats exacts à moins de  $\pm 20$  pour cent près.

## MANAGEMENT PERSPECTIVE

The Water Survey of Canada has been looking for a method in which their Hydac 200 hydrographic survey system can be used for the measurement of bed load in alluvial rivers. In response to this need, the Hydraulics Division conducted a study and developed an equation which can be used to compute bed load from bed profile records of migrating dunes. The equation, presented by Engel and Lau, contains a bed-load coefficient whose value depends on the flow pattern near the dunes. Specifically, the stagnation point on the upstream face of the bed form has to be located. Previously, this location could only be estimated from some published data which then resulted in a particular value for the bed-load coefficient.

This report presents the result of a systematic study to define the location of the stagnation point and how it varies with dune profile and other flow variables. Using this information, the bed-load coefficient can now be chosen for the particular field condition encountered. This will increase the accuracy of the computation of bed load using profile records.

T. M. Dick  
Chief  
Hydraulics Division  
June 6, 1980



## PERSPECTIVE DE GESTION

La Division des relevés hydrologiques du Canada recherche une méthode qui permette de recourir à son système Hydrac 200 de relevés hydrographiques pour mesurer le charriage de fond des rivières alluviales. Pour répondre à ce besoin, la Division d'hydraulique a effectué une étude et formulé une équation pouvant servir à calculer le charriage de fond à partir du relevé des profils de fond des dunes en migration. Présentée par Engel et Lau, l'équation fait état d'un coefficient de charriage de fond dont la valeur dépend du modèle d'écoulement près des dunes. Plus précisément, il faut localiser le point de stagnation sur la face amont de la configuration du fond. Auparavant, le seul moyen d'évaluer cet emplacement, c'était de se reporter à des données publiées, ce qui donnait une certaine valeur pour le coefficient de charriage de fond.

Le présent rapport présente le résultat d'une étude systématique pour définir l'emplacement du point de stagnation et sa variation selon le profil de la dune et d'autres variables du débit. Grâce à ces renseignements, on peut maintenant choisir le coefficient de charriage de fond pour les conditions particulières rencontrées sur le terrain. On pourra ainsi accroître l'exactitude des calculs de charriage de fond à partir des relevés de profils.

T. M. Dick

Chef

Division de l'hydraulique

Le 6 juin 1980

Open-channel flow over a mobile bed is a complex process because of the interrelationship between the fluid and the bed. When the flow is tranquil (Froude No.  $< 1$ ), the water deforms the bed into ripples or dunes depending on the flow conditions and the grain size of the bed. In return the deformed bed affects the flow through its increase on flow resistance. As the flow passes over the bed forms, a separation occurs at the crests, creating a wake zone or zone of separation which extends some distance downstream to the point of reattachment on the back of the next bed form. Within these separation zones, reverse circulations exist which are produced by the turbulent generation of vortices originating at the interface between the main flow and the wake zone. This results in a velocity along the bed in the upstream direction within this zone. As a result the bed material in this region remains either in situ or tends to move in an upstream direction depending on the intensity of the reverse flow at the bed. This means that the material contributing to the average bed-load discharge must be obtained from the region between the point of flow reattachment and the first crest downstream. This contention is supported by observations of Raudkivi (1963), Sheen (1964), Vanoni and Hwang (1967), Raudkivi and Sheen (1976) and Etheridge and Kemp (1978).

The fact that bed-load transport occurs only between the point of flow reattachment and the next crest, was a basic consideration in the development of an equation by Engel and Lau (1980) to compute bed load from bed profile records of migrating dunes. A basic requirement of this equation is a definition of the bed elevations on the bed forms at which there is zero transport and this was taken to be at the point of flow reattachment. Analysis of data by Jonys (1973) for a large number of dunes showed that the point of maximum pressure (minimum velocity) could be taken above the trough elevation in the lee of the bed forms by an amount equal to 0.17 the bed-form height.

A review of the literature could not confirm the above value for the position of zero transport nor was it possible to determine this position theoretically. Therefore, an experimental study was conducted to reveal the relationship between the position of zero transport, bed-form height, bed-form shape, grain size and flow conditions. The results are used to produce a bed-load discharge coefficient for use with the equation presented by Engel and Lau (1980). This study is part of the environmental hydraulics programme under study number H79-013.

## 2.0 LITERATURE REVIEW

A search of the literature indicated that there was no information available on the elevation of the point of zero transport for flows over ripples or dunes. Therefore, the search was concentrated to obtain information which would make it possible to define this critical point by indirect means.

Since the position of zero transport is taken to be at the point of flow reattachment, then this position can be readily obtained from knowledge of the length of the separation zone and the bed-form geometry. Raudkivi (1963) found that "... at six times the ripple height downstream from the crest there was a hesitancy in the grain movement in that some grains were moving forward and others backward". Walker (1961) measured the separation length behind a rearward facing rectangular step and found it to be slightly greater than about five times the step height. Measurements by Etheridge and Kemp (1978), also over a rearward facing step showed that the ratio of length of the separation zone to height of step varied between 5 and 7. However, their measurements were made without the "... basic conditions of constant Reynolds number, Froude number and upstream flow conditions being fulfilled". This latter restriction considerably limits the usefulness of their results for defining the separation length as a function of flow conditions, especially, since their data showed that the separation length to step-height ratio was not constant. Chang (1970) measured the length of the separation zone behind a single cast iron angle placed on a plane bed in a rectangular flume, repeating his tests for three different sizes of angles for different flow conditions. He found that the ratio of the separation length to angle height varied with flow velocity from 5 to 8. Knoroz (1959), in developing an equation for the friction factor for dune beds, determined that the length of the separation zone is ten times the dune height. Examination of data from Jonys (1973) indicated that for his dunes the length of the separation zone, on the average, is about five times the dune height.

The results from the literature indicate that the length of the separation zone for dunes can vary from about five (Jonys, 1973) to ten (Knoroz, 1959) times the height of the dunes but the information is too limited to determine any kind of relationship between length of separation to bed-form height ratio, the bed-form shape and flow conditions. The results from measurements over ripples and rearward facing steps appear to yield similar ratios of separation length to object height. However, it is doubtful that this

similarity can be taken to be general, especially if the ripples and dunes have steep upstream faces. The most systematic and extensive tests were those of Chang (1970) but it is not likely that the flows over a single cast iron angle can be taken as being representative of flow over bed forms. Indeed, Morris (1959) states that roughness spacing is important and that the shape of the wake zone should depend on the shape of the roughness elements.

In view of the limited available information, it is necessary to conduct a set of experiments in order to provide the necessary data from which a satisfactory definition of the zero transport position on the bed forms can be obtained.

### 3.0 ANALYTICAL CONSIDERATIONS

#### 3.1 Background

The equation developed by Engel and Lau (1980) to compute bed-load discharge from migrating dunes is given by

$$G_s = 1.32 \gamma_s (1-P) \bar{\xi} U_w \quad 3.1$$

where  $G_s$ =submerged weight of bed load per unit width per unit times,  $\gamma_s$ =submerged unit weight of sediment,  $P$ =porosity of sediment,  $\bar{\xi}$ =average departure of the bed elevations about the average of all the elevation  $\bar{\eta}$  in the profile record and  $U_w$ =speed of the migrating dunes. In developing equation 3.1, it was assumed that the dunes were triangular in shape. An additional requirement was to define the distance between the elevation of zero transport  $\eta_o$  and the lowest point in the trough  $\eta_t$  for the dunes (Figure 1). From data by Jonys (1973), an average value of this distance in terms of dune height  $\Delta$  was determined as  $(\bar{\eta}_o - \eta_t) = 0.17 \Delta$ . This value together with the assumption of triangular dune shapes was fundamental to the final value of 1.32 given in equation 3.1. Reasonably good results were obtained when bed-load discharge computed with equation 3.1 was compared with data from flume experiments.

#### 3.2 Bed Load Discharge Coefficient

The coefficient of 1.32 in equation 3.1 may be regarded as a particular value of a general bed-load coefficient, which may be obtained from a derivation by Engel and Lau (1980), by writing

$$K = a (\alpha - k) \quad 3.2$$

where  $a$ ,  $\alpha$  and  $k$  are coefficients. Values of  $a$  and  $\alpha$  depend upon the shape of the dunes.  $\alpha$  represents the fraction of the height of the rectangle, with a base equal to the dune length  $\Lambda$  and an area equal to the longitudinal cross-sectional area of a dune, to the height of the dune  $\Delta$ . The coefficient "a" represents the ratio  $\Delta/\bar{\xi}$ . The coefficient  $k$  represents the ratio of  $(\bar{\eta}_o - \eta_t)/\Delta$  which can be expected to vary with flow conditions, bed-form steepness and grain size of the bed material. For a triangular dune shape  $\alpha=0.5$  and  $a=4$ . Fredsøe (1979) found in

studying dune shape parameters that the triangular shape is more correct than a sinusoidal form. Willis and Kennedy (1977) state that the assumption of triangular dunes is sufficiently accurate for computation of bed-load transport rates. Therefore, the triangular dune shape was used for this study and the bed-load discharge coefficient K may be written as

$$K = 4 \left[ 0.5 - k \right] \quad 3.3$$

By keeping  $a$  and  $\alpha$  constant at 4 and 0.5 respectively, it is possible to reveal the effect of  $k$  on the computation of bed-load discharge with equation 3.1.

### 3.3 Dimensional Analysis

In order to have good control of the variables defining the dune height and length, it is convenient to use a rigid bed composed of artificial dunes. Under these conditions, considering two-dimensional flow in a straight uniform channel,  $k$  can be expressed as

$$k = f \left[ \Delta, \Lambda, \phi, D_{50}, h, U, \rho, \mu, g \right] \quad 3.4$$

where  $\Lambda$ =length of bed forms (crest to crest),  $\Delta$ =height of dunes (trough to crest),  $\phi$ =angle of inclination of downstream face of dunes,  $D_{50}$ =median grain diameter,  $h$ =average depth of flow,  $U$ =average flow velocity,  $\rho$ =density of the fluid,  $\mu$ =viscosity of the fluid and  $g$ =acceleration due to gravity. The symbols are schematically defined in Figure 1. Using the  $\pi$  theorem for dimensional analysis and simplifying, equation 3.4 can be written in dimensionless form as

$$k = f_1 \left[ \frac{\Delta}{\Lambda}, \phi, \frac{D_{50}}{\Delta}, \frac{h}{\Delta}, \frac{U \Delta \rho}{\mu}, \frac{U}{\sqrt{gh}} \right] \quad 3.5$$

Measurements by Etheridge and Kemp (1978) have shown that flow in the separation zone is insensitive to the flow in the corner region at the foot of a reverse rectangular step. This suggests that quite crude modelling of ripples and dunes in the region between crest and downstream toe is justifiable. Therefore, the angle  $\phi$  is not an important parameter in equation 3.4 and can be omitted from further consideration. For large Reynolds number, the effect of viscosity will also not be important and the term  $U \Delta \rho / \mu$  can be deleted. The relationship which is being sought is then

$$k = f_2 \left[ \frac{\Delta}{\Lambda}, \frac{D_{50}}{\Delta}, \frac{h}{\Delta}, \frac{U}{\sqrt{gh}} \right]$$

3.6

Experiments were conducted to investigate the variation of  $k$  with the independent variables.

**EXPERIMENTAL EQUIPMENT AND PROCEDURE**

Experiments were conducted in a tilting flume rectangular in cross-section, 20 metres long and 1-metre wide. Discharges were measured at the downstream end using a weir box. The flow leaving the flume was split into three parts of equal width and only the flow from the central portion was measured in the weir box. By working only with the nearly two-dimensional flow in the centre portion of the flume, the effect of the side walls was practically eliminated. The flows were always uniform with Froude numbers not exceeding 0.5.

The dune roughness was obtained by using artificial bed forms fabricated from plywood and covered with sand. Four different bed form shapes ( $\Delta/\Lambda$ ), each with different sand roughnesses ( $D_{50}$ ), as well as the smooth bed forms ( $D_{50}=0$ ) were used. All bed forms had a height of 3 cm with a downstream toe angle of  $\phi=30^\circ$  and were placed over the full length of the flume. The sand was fixed to the bed forms by first covering these with "Mactac", self adhesive vinyl covering. Then a thin layer of varnish was brushed on and the sand was sprinkled on top so that the "Mactac" was completely covered (Lau, Krishnappan, 1977). After drying overnight, the excess sand was washed off and a uniform layer of sand was left on the dunes. To change over to another sand roughness, the "Mactac" was stripped off and the process repeated. Each bed form was tested with one or more sand sizes before a new one was placed in the flume. In all, three different sand sizes were used having median diameters of 0.62 mm, 1.20 mm, and 2.60 mm, thus each sand size was approximately twice as large as the one preceding it. Tests on the plane bed forms were conducted using the smooth surface of the "Mactac" only.

The values of  $k$  were obtained by measuring the length of the flow separation  $l_w$  (Figure 1) using a Potassium Permanganate dye as a visual aid. A 100 ml hypodermic syringe with a needle 45 cm long and 1 mm inside diameter was attached to a traversing mechanism on a movable carriage which travelled on the rails on top of the flume walls. This permitted movement of the syringe in both the vertical and horizontal direction (Figure 2). The tip of the hypodermic needle was ground off at an angle of  $30^\circ$  with the vertical. This made it possible to place the needle so that the dye was always injected into the flow at right angles to the main flow, and ensured that no momentum in the



streamwise direction was imparted to the dye. Once a given flow was set up the syringe was filled with the dye and positioned on the centreline of the flow and then lowered so that the needle was about 1 mm or less above the dune surface.

The location of the point of flow reattachment was obtained by the following two steps. In both steps, dye was injected into the flow in small short pulses and these were observed to note their direction of movement. In the first step, the syringe was always positioned well downstream of the anticipated separation zone so that there was a clear and distinct movement of dye pulses downstream (Figure 3a). The syringe was then moved in small increments to new positions upstream and in each case the behaviour of the dye pulses was carefully noted. The progressive upstream positioning continued until it was observed that some of the dye tended to travel upstream. This point was defined as the downstream edge of the region in which the point of flow reattachment occurs. The concept of a region was adopted since, due to the turbulent fluctuations, it would not be possible to define a precise point, but rather an average. In the second step of the procedure, the syringe was placed at the toe of the bed form in the separation zone being considered. At this point, the dye pulses clearly moved upstream and up the steep face of the dune. The syringe was then placed at different positions, each being about 3 to 4 mm further downstream than the previous one, and the movement of the dye observed (Figure 3b). This was continued until once again a portion of the dye pulse was entrained in the downstream flow. This point was taken to be the upstream edge of the region for the point of flow reattachment. All positional measurements were related to the crest of the dune upstream of the separation zone and thus the probable average location of the point of flow reattachment was simply the average of the measurement pairs. Several pairs of such measurements were made for a given flow condition to ensure a reasonably reliable average position for the point of flow reattachment. Values of  $k$  were computed from the measured  $l_w$  values by using the formula

$$k = \frac{\frac{l_w}{\Delta} - \cot \phi}{\frac{l}{\Delta/\Lambda} - \cot \phi} \quad 4.1$$

The data from the experiments together with the computed values of  $k$  are given in Table 1.

## 5.0 DATA ANALYSIS

Values of  $k$  were plotted versus the Froude number  $U/\sqrt{gh}$  for each dune shape  $\Delta/\Lambda$  using  $h/\Delta$  as a parameter for each given value of  $D_{50}/\Delta$  in Figures 4, 5, 6, and 7. In all cases, it is clear that, within the experimental error,  $k$  is virtually independent of the Froude number. It is also apparent from the plots that  $k$  is, at most, only weakly dependent on  $h/\Delta$  but that values of  $k$  tend to decrease as  $D_{50}/\Delta$  increases. In all cases, depths of flow were chosen so as to encompass the depths for which  $\Lambda/h=2\pi$  and  $\Lambda/h=5$ . Yalin (1977) has shown that in the presence of dunes  $\Lambda/h=2\pi$  when  $U_*D_{50} \rho/\mu$  ( $U_*$ =shear velocity)  $> 40$  and Ashida and Kishi (1974) have shown that  $\Lambda/h=5$  when  $U_*D_{50} \rho/\mu > 0$ . Since  $U/\sqrt{gh}$  and  $h/\Delta$  are shown to be, at best, weakly significant in the dune regime, these terms can be omitted from further consideration. Therefore, the data analysis can be reduced to revealing the form of the relationship

$$k = f_3 \left[ \frac{\Delta}{\Lambda}, \frac{D_{50}}{\Delta} \right] \quad 5.1$$

Average values of  $k$  were obtained by fitting smooth straight lines through the plotted data of Figures 4, 5, 6, and 7. These values of  $k$  together with the corresponding values of  $\Delta/\Lambda$  and  $D_{50}/\Delta$  are given in Table 2. The values of  $k$  were then plotted as functions of  $D_{50}/\Delta$  using  $\Delta/\Lambda$  as a parameter in Figure 8. The data plot as a family of curves which over the range of the variables can be described quite well by straight lines. The slopes of the curves show that for small values of  $\Delta/\Lambda$  the effect of change in grain size is more significant than for larger values of  $\Delta/\Lambda$ . As values of  $\Delta/\Lambda$  increase from 0.02, the slopes of the lines progressively decrease until when  $\Delta/\Lambda=0.07$ , the slope may be considered to be negligible and  $k$  remains sensibly constant.

As the effect of  $\Delta/\Lambda$  is much greater than  $D_{50}/\Delta$  as shown by the spacing between the curves in Figure 8, then a more useful plot is to use  $D_{50}/\Delta$  as a parameter. This plot is shown in Figure 9. The variation of  $k$  is now shown as a family of curves which diverge in a nonlinear fashion from a common value for  $\Delta/\Lambda=0.07$  to form separate branches for each value of  $D_{50}/\Delta$  as  $\Delta/\Lambda$  decreases toward  $\Delta/\Lambda=0.02$ . The rate of divergence clearly slows the effect of the grain size on the value of  $k$  as  $\Delta/\Lambda$  becomes smaller.

Next, values of  $k$  were obtained for even values of  $D_{50}/\Delta$  for each value of  $\Delta/\Lambda$  from Figure 8 and these were used to compute values of  $K$  given by

equation 3.2 for the case of  $a=4$  and  $\alpha=0.5$ . The values of  $K$  are given in Table 3 and were plotted in Figure 10 as a function  $\Delta/\Lambda$  using  $D_{50}/\Delta$  as a parameter. The family of curves displays similar characteristics as that of Figure 9 except that  $K$  decreases as  $\Delta/\Lambda$  increases which is a direct consequence of the application of  $k$  to equation 3.2

Upon examining Figure 10, it is interesting to note that when  $\Delta/\Lambda=0.06$ ,  $k=0.17$  which is the value used by Engel and Lau (1980) to obtain the value of  $K=1.32$  in Figure 10. The value of  $\Delta/\Lambda=0.06$  is the maximum value that is likely to occur for dunes (Yalin, 1977) and is approximately the value for the data of Jonys (1973) used by Engel and Lau (1980). Therefore, one would expect that, in the dune regime, the working range of  $K$  should be  $0.02 < \Delta/\Lambda < 0.06$ . In this range of  $\Delta/\Lambda$ , it can be seen from Figure 10 that there is always an effect on  $K$  due to the size of the sand grains on the bed. For the case of  $\Delta/\Lambda=0.06$ , this effect is very small but this increases significantly as  $\Delta/\Lambda$  decreases to the lower end of the working range.

Having determined the variation of  $k$  in equation 5.1, one can now combine equation 3.3 and 5.1 to obtain the general bed-load discharge coefficient as

$$K = \left[ 2.0 - 4 f_3 \left( \frac{\Delta}{\Lambda}, \frac{D_{50}}{\Delta} \right) \right] = K \left[ \frac{\Delta}{\Lambda}, \frac{D_{50}}{\Delta} \right] \quad 5.2$$

## APPLICATION OF THE BED-LOAD COEFFICIENT

Existing data used by Engel and Lau (1980) was used as a preliminary test to assess the effect of using K from equation 5.2 when computing bed-load discharge with the "Hydrographic Method". These data are given in Table 4. Values of K were then obtained for the appropriate values of  $\Delta/\Lambda$  and  $D_{50}/\Delta$  for each of the ten runs and the bed-load discharge  $G_{sc}$  computed. These computed values of  $G_{sc}$  were compared with the measured values  $G_{sm}$  by computing the relative percent error defined as

$$E = \frac{G_{sc} - G_{sm}}{G_{sc}} \times 100 \% \quad 6.1$$

The computed values of  $G_{sc}$  and E are given also in Table 4. In order to assess the effect of K, the computed bed-load discharge errors in Table 4 were compared with the percent errors obtained by Engel and Lau (1980) when  $K=1.32$ . The computed bed-load discharge and the corresponding percent errors for the two cases of K are given in Table 5.

The values of the computed bed load were plotted versus the measured transport rate for the two cases of  $K=1.32$  and  $K=K\left[\Delta/\Lambda, D_{50}/\Delta\right]$  in Figure 11. Upon comparing the two sets of plotted data, it can be seen that the effect of  $K=K\left[\Delta/\Lambda, D_{50}/\Delta\right]$  has been to reduce the negative errors and to increase the positive errors over the range of  $\Delta/\Lambda$  from .039 to .062 used. However, the reduction in the negative errors was greater than the increase in the positive errors. The net effect of this was a change in overall average error from -5.2 percent to +3.6 percent. The overall average absolute error changed from 15.2 percent to 14.5 percent.

The use of the bed-load coefficient  $K=K\left[\Delta/\Lambda, D_{50}/\Delta\right]$  has resulted in an overall improvement. However, the limited data indicates that the improvement is small because the value of K depends heavily on the bed-form parameters  $\Delta$  and  $\Lambda$  both of which are known to have large sampling variances. This is particularly true for the bed-form height  $\Delta$ . Since it has been shown in Figure 10 that K is quite sensitive to changes in  $\Delta/\Lambda$ , then it is quite clear that values of K cannot be more reliable than the measured values of  $\Delta$  and  $\Lambda$ . Consequently, it appears that unless the measurements of bed-form steepness are improved, the best one can expect is to compute the bed load with an error of the order of  $\pm 20$  percent.

## 7.0

### CONCLUSIONS

1. The position of zero transport on the back of a dune varies with the steepness of the dunes and the grain size of the bed material and is independent of depth of flow and the Froude number.
2. The bed-load coefficient is quite sensitive to changes in dune steepness and to a lesser degree to changes in grain size of the bed material. When dunes are flat the effect of sand size on the bed-load coefficient is significant. When dunes are steep, the coefficient depends on dune steepness only.
3. The use of the bed-load coefficient resulted in some improvement by decreasing the overall average error in a set of ten separate flume tests.
4. The value of the bed-load coefficient or  $K=1.32$  used by Engel and Lau (1980) appears to be a special case representing the value for maximum dune steepness of 0.06.
5. Because the bed-load coefficient is difficult to obtain with great precision, a realistic error in the estimate of bed-load transport is  $\pm 20$  percent of the true value. An error nevertheless which is a significant improvement over estimates from theory.

## REFERENCES

- Ashida, R. and Kishi, T., 1974. "The Bed Configuration and Roughness of Alluvial Streams". Task Committee on Bed Configurations and Hydraulic Resistance of Alluvial Streams, Committee on Hydraulics and Hydraulic Engineering, Japan Society of Civil Engineers, Tokyo, 160, Japan.
- Chang, F.F.M., 1970. "Ripple Concentration and Friction Factor". Proc. ASCE, Vol. 96 HY2.
- Crickmore, M. G., 1970. "Effect of Flume Width on Bed-Form Characteristics". Proc. ASCE, Vol. 96, HY2.
- Engel, P. and Lau, Y. L., 1980. "Computation of Bed Load using Bathymetric Data". ASCE, Journal of the Hydraulics Division, Proc. ASCE, Vol. 106, HY3.
- Etheridge, D. W. and Kemp, P. H., 1979. "Velocity Measurements Downstream of Rearward Facing Steps, with Reference to Bed Instability". Jour. of Hydraulic Research, IAHR, Vol. 17, No. 2.
- Fredsoe, J., 1979. "Dimensions of Stationary Dunes". Progress Report HY9, pp 3-10, August, Inst. Hydrodyn. and Hydr. Engrg., Tech. Univ. Denmark.
- Jonys, C. K., 1973. "An Experimental Study of Bed-Form Mechanics". Thesis in partial fulfillment of the requirements for degree of Doctor of Philosophy, Dept. of Civil Engineering, University of Alberta, Canada.
- Knoroz, U.S., 1959. "The Effect of the Channel Macro Roughness on its Hydraulic Resistance". Ozvesticia Vsesoiuznogo Nanchno-Ossledovatel'kogo, Instituta, Gidrotekhniki, Vol. 62, pp. 75-96, Translated by I. Mitten, USGS.
- Lau, Y. L. and Krishnappan, B. G., 1979. "Transverse Dispersion in Rectangular Channels". Proc. ASCE, Vol. 103, HY10.
- Morris, H. M., 1959. "Design Methods for Flow in Rough Conduits". Proc. ASCE, Vol. 85, HY7.
- Raudkivi, A. Y., 1963. "Study of Sediment Ripple Formation". Proc. ASCE, Vol. 89, HY6.
- Raudkivi, A. Y., 1976. "Loose Boundary Hydraulics". Second Edition, Pergamon Press, Oxford.
- Sheen, S. J., 1964. "Turbulence over a Sand Ripple". Master of Engineering Thesis, University of Auckland, New Zealand.

Vanoni, V. A. and Hwang, L. S., 1967. "Relation between Bed-Forms and Friction in Streams". Proc. ASCE, Vol. 95, HY4.

Walker, G. R., 1961. "A Study of the Two-Dimensional Flow of Turbulent Fluid Past a Step". Master of Engineering Thesis, University of Auckland, New Zealand.

Yalin, M. S., 1977. "Mechanics of Sediment Transport". Second Edition, Pergamon Press.

## ACKNOWLEDGEMENTS

All the measurements and photographs were made by Mr. J. Dalton assisted by Mr. D. Doede. The writer is grateful for their dedication to this project.



TABLE 1

## EXPERIMENTAL DATA

Run No.	D <sub>50</sub> mm	h cm	U cm/s	$\frac{h}{w}$ cm	$\frac{h}{\Delta}$	$\frac{D_{50}}{\Delta}$	$\frac{\Delta}{\lambda}$	$\frac{U}{\sqrt{gh}}$	k
1	0	30	30.75	13.97	10.0	0	0.033	.179	.103
2	0	30	54.96	14.00	10.0	0	0.033	.320	.103
3	0	30	70.09	13.80	10.0	0	0.033	.409	.100
4	0	30	60.41	13.87	10.0	0	0.033	.352	.101
5	0	30	50.88	14.17	10.0	0	0.033	.297	.105
6	0	30	42.66	14.53	10.0	0	0.033	.249	.108
7	0	30	42.94	14.33	10.0	0	0.033	.250	.107
8	0	30	49.95	14.07	10.0	0	0.033	.288	.104
9	0	30	63.85	14.98	10.0	0	0.033	.372	.114
10	0	30	71.75	14.57	10.0	0	0.033	.418	.110
11	0	30	13.70	14.53	10.0	0	0.033	.080	.109
12	0	20	40.99	13.90	6.7	0	0.033	.293	.101
13	0	20	55.05	14.01	6.7	0	0.033	.393	.103
14	0	20	70.45	14.37	6.7	0	0.033	.503	.107
15	0	20	52.03	14.17	6.7	0	0.033	.372	.105
16	0	20	37.43	14.77	6.7	0	0.033	.267	.112
17	0	20	29.28	14.75	6.7	0	0.033	.209	.112
18	0	20	36.29	14.37	6.7	0	0.033	.259	.107
19	0	43	19.25	14.35	14.3	0	0.033	.094	.107
20	0	43	24.60	14.08	14.3	0	0.033	.120	.104
21	0	43	31.79	14.40	14.3	0	0.033	.155	.107
22	0	43	34.95	14.68	14.3	0	0.033	.170	.111
23	0	43	57.31	14.75	14.3	0	0.033	.279	.112
24	0	43	82.59	14.68	14.3	0	0.033	.402	.111
25	2.6	20	25.19	13.18	6.7	0.087	0.033	.180	.093
26	2.6	20	30.51	13.25	6.7	0.087	0.033	.218	.094
27	2.6	20	37.43	12.93	6.7	0.087	0.033	.267	.090
28	2.6	20	41.90	13.03	6.7	0.087	0.033	.299	.091
29	2.6	20	52.80	12.50	6.7	0.087	0.033	.377	.085
30	2.6	20	58.72	12.68	6.7	0.087	0.033	.419	.087
31	2.6	20	67.20	12.70	6.7	0.087	0.033	.480	.088
32	2.6	20	46.88	12.85	6.7	0.087	0.033	.335	.089
33	2.6	30	15.61	12.53	10.0	0.087	0.033	.091	.086
34	2.6	30	20.50	12.40	10.0	0.087	0.033	.120	.084
35	2.6	30	24.72	12.38	10.0	0.087	0.033	.144	.084
36	2.6	30	29.77	12.68	10.0	0.087	0.033	.174	.087
37	2.6	30	34.43	12.83	10.0	0.087	0.033	.201	.089
38	2.6	30	37.75	13.10	10.0	0.087	0.033	.220	.092
39	2.6	30	41.37	12.90	10.0	0.087	0.033	.241	.090
40	2.6	30	44.80	12.88	10.0	0.087	0.033	.261	.090
41	2.6	43	14.23	13.43	14.3	0.087	0.033	.069	.096
42	2.6	43	17.66	13.40	14.3	0.087	0.033	.086	.096
43	2.6	43	21.63	12.98	14.3	0.087	0.033	.105	.091
44	2.6	43	24.24	13.03	14.3	0.087	0.033	.118	.091
45	2.6	43	27.03	13.05	14.3	0.087	0.033	.132	.092

TABLE 1 cont.

## EXPERIMENTAL DATA

Run No.	D <sub>50</sub> mm	h cm	U cm/s	ℓ <sub>w</sub> cm	$\frac{h}{\Delta}$	$\frac{D_{50}}{\Delta}$	$\frac{\Delta}{\Lambda}$	$\frac{U}{\sqrt{gh}}$	k
46	2.6	43	28.20	13.28	14.3	0.087	0.033	.137	.094
47	2.6	43	32.42	12.88	14.3	0.087	0.033	.158	.090
48	2.6	43	36.76	13.23	14.3	0.087	0.033	.179	.094
49	1.2	30	16.12	13.40	10.0	0.040	0.033	.094	.096
50	1.2	30	25.84	13.90	10.0	0.040	0.033	.151	.102
51	1.2	30	31.51	14.23	10.0	0.040	0.033	.184	.105
52	1.2	30	44.45	13.67	10.0	0.040	0.033	.259	.099
53	1.2	30	48.02	13.33	10.0	0.046	0.033	.280	.095
54	1.2	30	53.42	13.60	10.0	0.040	0.033	.311	.098
55	1.2	43	14.12	13.45	14.3	0.040	0.033	.069	.096
56	1.2	43	17.57	13.45	14.3	0.040	0.033	.086	.096
57	1.2	43	22.11	13.18	14.3	0.040	0.033	.108	.093
58	1.2	43	25.79	13.13	14.3	0.040	0.033	.126	.093
59	1.2	43	29.86	13.13	14.3	0.040	0.033	.145	.093
60	1.2	43	35.75	13.15	14.3	0.040	0.033	.174	.093
61	1.2	43	40.99	13.08	14.3	0.040	0.033	.200	.092
62	1.2	43	45.84	13.10	14.3	0.040	0.033	.223	.092
63	1.2	43	53.15	13.15	14.3	0.040	0.033	.259	.093
64	1.2	20	37.61	14.03	6.7	0.040	0.033	.269	.103
65	1.2	20	46.98	14.20	6.7	0.040	0.033	.335	.105
66	1.2	20	29.36	13.58	6.7	0.040	0.033	.210	.098
67	1.2	20	32.52	13.90	6.7	0.040	0.033	.232	.102
68	1.2	20	37.78	14.15	6.7	0.040	0.033	.270	.105
69	1.2	20	41.44	13.80	6.7	0.040	0.033	.296	.100
70	0	20	21.15	12.68	6.7	0	0.070	.150	.199
71	0	20	36.45	12.65	6.7	0	0.070	.260	.198
72	0	20	38.95	12.68	6.7	0	0.070	.278	.199
73	0	20	55.95	12.88	6.7	0	0.070	.399	.204
74	0	20	63.89	12.35	6.7	0	0.070	.456	.190
75	0	20	25.98	12.92	6.7	0	0.070	.186	.205
76	0	20	45.20	12.63	6.7	0	0.070	.323	.198
77	0	20	50.10	12.38	6.7	0	0.070	.358	.191
78	0	30	22.80	12.60	10.0	0	0.070	.133	.197
79	0	30	30.51	12.30	10.0	0	0.070	.178	.189
80	0	30	52.22	12.75	10.0	0	0.070	.304	.201
81	0	30	77.95	12.48	10.0	0	0.070	.454	.194
82	0	30	60.30	12.60	10.0	0	0.070	.351	.197
83	0	43	11.57	12.68	14.3	0	0.070	.056	.199
84	0	43	19.86	12.80	14.3	0	0.070	.097	.202
85	0	43	45.62	12.95	14.3	0	0.070	.222	.206
86	2.6	30	21.06	12.60	10.0	0.087	0.050	.123	.135
87	2.6	30	26.85	12.98	10.0	0.087	0.050	.157	.142
88	2.6	30	32.13	12.60	10.0	0.087	0.050	.187	.135
89	2.6	30	40.69	12.95	10.0	0.087	0.050	.237	.142
90	2.6	30	45.22	12.88	10.0	0.087	0.050	.264	.140

TABLE 1 cont.

## EXPERIMENTAL DATA

Run No.	D <sub>50</sub> mm	h cm	U cm/s	ℓ <sub>w</sub> cm	$\frac{h}{\Delta}$	$\frac{D_{50}}{\Delta}$	$\frac{\Delta}{\Lambda}$	$\frac{U}{\sqrt{gh}}$	k
91	2.6	30	53.71	12.30	10.0	0.087	0.050	.313	.130
92	2.6	30	58.23	11.88	10.0	0.087	0.050	.339	.122
93	2.6	30	61.78	12.08	10.0	0.087	0.050	.360	.126
94	2.6	30	69.93	12.90	10.0	0.087	0.050	.408	.141
95	2.6	20	22.65	13.15	6.7	0.087	0.050	.162	.145
96	2.6	20	28.22	12.73	6.7	0.087	0.050	.201	.137
97	2.6	20	40.27	13.33	6.7	0.087	0.050	.287	.148
98	2.6	20	67.30	13.90	6.7	0.087	0.050	.480	.159
99	2.6	20	49.34	13.50	6.7	0.087	0.050	.352	.152
100	0	20	29.61	13.38	6.7	0	0.050	.211	.149
101	0	20	38.31	13.13	6.7	0	0.050	.274	.145
102	0	20	45.76	12.88	6.7	0	0.050	.327	.146
103	0	20	54.17	12.55	6.7	0	0.050	.387	.134
104	0	20	66.89	13.08	6.7	0	0.050	.478	.144
105	0	20	33.28	12.95	6.7	0	0.050	.238	.142
106	0	20	27.01	12.98	6.7	0	0.050	.193	.142
107	0	20	22.42	12.95	6.7	0	0.050	.160	.142
108	0	20	19.45	13.30	6.7	0	0.050	.139	.148
109	0	30	38.75	13.25	10.0	0	0.050	.226	.147
110	0	30	53.64	12.90	10.0	0	0.050	.313	.141
111	0	30	71.60	12.68	10.0	0	0.050	.417	.137
112	1.2	30	18.17	12.90	10.0	0.040	0.050	.106	.141
113	1.2	30	22.02	12.98	10.0	0.040	0.050	.128	.142
114	1.2	30	25.48	13.18	10.0	0.040	0.050	.149	.146
115	1.2	30	31.63	13.33	10.0	0.040	0.050	.184	.148
116	1.2	30	38.21	13.08	10.0	0.040	0.050	.223	.144
117	1.2	30	44.52	12.85	10.0	0.040	0.050	.260	.140
118	1.2	30	51.75	12.45	10.0	0.040	0.050	.302	.132
119	1.2	30	75.77	12.83	10.0	0.040	0.050	.442	.140
120	1.2	30	64.85	12.73	10.0	0.040	0.050	.378	.137
121	1.2	30	18.06	14.35	10.0	0.040	0.020	.105	.063
122	1.2	30	24.14	14.93	10.0	0.040	0.020	.141	.067
123	1.2	30	26.97	14.60	10.0	0.040	0.020	.157	.065
124	1.2	30	30.07	14.83	10.0	0.040	0.020	.175	.067
125	1.2	30	33.53	14.23	10.0	0.040	0.020	.195	.062
126	1.2	30	38.08	13.83	10.0	0.040	0.020	.222	.060
127	1.2	30	41.57	14.20	10.0	0.040	0.020	.242	.062
128	1.2	30	45.56	14.80	10.0	0.040	0.020	.266	.066
129	1.2	30	49.95	14.45	10.0	0.040	0.020	.291	.064
130	1.2	30	55.92	13.68	10.0	0.040	0.020	.326	.059
131	1.2	30	58.53	13.48	10.0	0.040	0.020	.341	.057
132	1.2	30	65.08	14.03	10.0	0.040	0.020	.379	.061
133	1.2	30	67.34	14.88	10.0	0.040	0.020	.393	.067
134	1.2	30	70.88	14.65	10.0	0.040	0.020	.413	.065

TABLE 1 cont.

## EXPERIMENTAL DATA

Run No.	$D_{50}$ mm	h cm	U cm/s	$l_w$ cm	$\frac{h}{\Delta}$	$\frac{D_{50}}{\Delta}$	$\frac{\Delta}{\Lambda}$	$\frac{U}{\sqrt{gh}}$	k
135	1.2	24	24.54	14.73	8.0	0.040	0.020	.160	.066
136	1.2	24	29.31	15.13	8.0	0.040	0.020	.191	.069
137	1.2	24	33.41	15.25	8.0	0.040	0.020	.218	.069
138	1.2	24	37.59	15.00	8.0	0.040	0.020	.245	.068
139	1.2	24	42.71	14.98	8.0	0.040	0.020	.278	.068
140	1.2	24	45.14	14.83	8.0	0.040	0.020	.294	.067
141	1.2	24	50.69	14.80	8.0	0.040	0.020	.330	.066
142	1.2	24	55.22	14.70	8.0	0.040	0.020	.360	.066
143	1.2	24	58.71	14.63	8.0	0.040	0.020	.360	.066
144	1.2	24	65.50	14.85	8.0	0.040	0.020	.383	.065
145	1.2	30	33.53	15.15	10.0	0.040	0.020	.195	.069
146	1.2	30	38.75	15.03	10.0	0.040	0.020	.226	.068
147	1.2	30	42.39	15.20	10.0	0.040	0.020	.247	.069
148	1.2	30	58.61	14.85	10.0	0.040	0.020	.342	.067
149	1.2	30	65.70	15.00	10.0	0.040	0.020	.383	.068
150	1.2	30	63.16	15.23	10.0	0.040	0.020	.368	.069
151	1.2	30	54.89	14.78	10.0	0.040	0.020	.368	.069
152	2.3	43	27.73	15.15	14.3	0.040	0.020	.135	.069
153	1.2	43	36.00	14.75	14.3	0.040	0.020	.175	.066
154	1.2	43	47.31	14.95	14.3	0.040	0.020	.230	.067
155	1.2	43	57.29	14.60	14.3	0.040	0.020	.250	.065
156	1.2	43	60.10	14.78	14.3	0.040	0.020	.293	.066
157	1.2	43	65.98	14.80	14.3	0.040	0.010	.321	.066
158	1.2	20	31.43	14.78	6.7	0.040	0.020	.224	.066
159	1.2	20	39.20	14.88	6.7	0.040	0.020	.280	.067
160	1.2	20	47.73	15.10	6.7	0.040	0.020	.341	.068
161	1.2	20	59.42	14.80	6.7	0.040	0.020	.424	.066
162	1.2	20	28.46	14.65	6.7	0.040	0.020	.203	.065
163	1.2	20	22.19	14.98	6.7	0.040	0.020	.158	.068
164	0	30	23.21	15.53	10.6	0	0.020	.135	.071
165	0	30	27.81	16.33	10.0	0	0.020	.162	.077
166	0	30	31.07	16.53	10.0	0	0.020	.181	.078
167	0	30	34.36	16.60	10.0	0	0.020	.200	.079
168	0	30	39.41	16.40	10.0	0	0.020	.230	.077
169	0	30	43.35	16.33	10.0	0	0.020	.253	.077
170	0	30	47.88	16.58	10.0	0	0.020	.279	.079
171	0	30	54.89	16.25	10.0	0	0.020	.320	.076
172	0	30	61.63	16.50	10.0	0	0.020	.359	.078
173	0	24	22.78	16.53	8.0	0	0.020	.148	.078
174	0	24	27.59	16.90	8.0	0	0.020	.180	.081
175	0	24	33.04	17.43	8.0	0	0.020	.215	.085
176	0	24	37.98	16.93	8.0	0	0.020	.248	.081
177	0	24	43.76	17.00	8.0	0	0.020	.285	.082
178	0	24	50.95	16.35	8.0	0	0.020	.332	.077

TABLE 1 cont.

## EXPERIMENTAL DATA

Run No.	$D_{50}$ mm	h cm	U cm/s	$l_w$ cm	$\frac{h}{\Delta}$	$\frac{D_{50}}{\Delta}$	$\frac{\Delta}{\Lambda}$	$\frac{U}{\sqrt{gh}}$	k
179	0	24	57.83	16.33	8.0	0	0.020	.377	.077
180	0	24	65.86	16.65	8.0	0	0.020	.429	.079
181	0	43	20.34	16.10	14.3	0	0.020	.099	.075
182	0	43	24.06	16.43	14.3	0	0.020	.117	.078
183	0	43	30.24	16.23	14.3	0	0.020	.147	.076
184	0	43	34.10	16.33	14.3	0	0.020	.166	.077
185	0	43	39.22	16.25	14.3	0	0.020	.191	.076
186	0	43	42.04	16.33	14.3	0	0.020	.205	.077
187	0	43	47.31	16.03	14.3	0	0.020	.230	.075
188	0	43	50.62	16.15	14.3	0	0.020	.246	.076
189	0	43	56.85	16.33	14.3	0	0.020	.277	.077
190	0	43	59.17	16.00	14.3	0	0.020	.288	.075
191	0	20	30.43	17.30	6.7	0	0.020	.217	.084
192	0	20	38.84	17.10	6.7	0	0.020	.277	.082
193	0	20	48.30	17.03	6.7	0	0.020	.345	.082
194	0	20	58.12	16.55	6.7	0	0.020	.415	.079
195	0	20	25.51	16.95	6.7	0	0.020	.182	.081
196	0	20	33.96	17.10	6.7	0	0.020	.242	.082
197	0	20	42.35	17.55	6.7	0	0.020	.302	.085
198	0	20	51.25	17.00	6.7	0	0.020	.366	.082
199	2.6	20	21.14	13.45	6.7	0.087	0.020	.151	.057
200	2.6	20	27.33	13.55	6.7	0.087	0.020	.195	.058
201	2.6	20	32.27	13.38	6.7	0.087	0.020	.230	.057
202	2.6	20	38.31	13.63	6.7	0.087	0.020	.274	.059
203	2.6	20	45.11	14.20	6.7	0.087	0.020	.322	.062
204	2.6	20	52.03	13.80	6.7	0.087	0.020	.371	.059
205	2.6	20	58.42	13.30	6.7	0.087	0.020	.471	.056
206	2.6	20	65.74	13.35	6.7	0.087	0.020	.469	.056
207	2.6	24	25.02	13.30	8.0	0.087	0.020	.163	.056
208	2.6	24	31.93	13.30	8.0	0.087	0.020	.208	.056
209	2.6	24	39.54	13.40	8.0	0.087	0.020	.258	.057
210	2.6	24	47.19	13.38	8.0	0.087	0.020	.308	.057
211	2.6	24	55.82	13.90	8.0	0.087	0.020	.364	.060
212	2.6	30	19.03	13.35	10.0	0.087	0.020	.111	.056
213	2.6	30	24.95	13.45	10.0	0.087	0.020	.145	.057
214	2.6	30	35.07	13.83	10.0	0.087	0.020	.204	.060
215	2.6	30	42.05	13.30	10.0	0.087	0.020	.245	.056
216	2.6	43	13.73	14.08	14.3	0.087	0.020	.077	.061
217	2.6	43	24.97	13.95	14.3	0.087	0.020	.140	.061
218	2.6	43	32.08	13.68	14.3	0.087	0.020	.156	.059
219	2.6	43	36.76	14.13	14.3	0.087	0.020	.207	.062
220	2.6	43	40.63	13.80	14.3	0.087	0.020	.228	.059
221	0.62	20	25.90	16.38	6.7	0.021	0.020	.185	.077
222	0.62	20	33.28	16.65	6.7	0.021	0.020	.238	.079

TABLE 1 cont.

## EXPERIMENTAL DATA

Run No.	D <sub>50</sub> mm	h cm	U cm/s	ℓ <sub>w</sub> cm	$\frac{h}{\Delta}$	$\frac{D_{50}}{\Delta}$	$\frac{\Delta}{\Lambda}$	$\frac{U}{\sqrt{gh}}$	k
223	0.62	20	43.17	16.40	6.7	0.021	0.020	.308	.077
224	0.62	20	50.97	16.48	6.7	0.021	0.020	.364	.078
225	0.62	20	63.17	17.03	6.7	0.021	0.020	.451	.082
226	0.62	20	57.12	16.55	6.7	0.021	0.020	.408	.078
227	0.62	20	22.27	16.45	6.7	0.021	0.020	.159	.078
228	0.62	30	30.69	16.70	10.0	0.021	0.020	.179	.080
229	0.62	30	22.64	16.48	10.0	0.021	0.020	.132	.079
230	0.62	30	35.72	16.90	10.0	0.021	0.020	.208	.081
231	0.62	30	38.08	16.30	10.0	0.021	0.020	.222	.077
232	0.62	30	45.15	15.90	10.0	0.021	0.020	.263	.074
233	0.62	30	48.52	15.98	10.0	0.021	0.020	.283	.075
234	0.62	30	51.39	15.95	10.0	0.021	0.020	.283	.075
235	0.62	30	55.55	16.05	10.0	0.021	0.020	.324	.075
236	0.62	30	58.38	15.93	10.0	0.021	0.020	.340	.074
237	0.62	30	37.95	16.15	10.0	0.021	0.020	.221	.076
238	0.62	30	29.40	16.80	10.0	0.021	0.020	.171	.080
239	0.62	43	27.07	16.25	14.3	0.021	0.020	.107	.076
240	0.62	43	28.67	16.25	14.3	0.021	0.020	.140	.076
241	0.62	43	35.35	16.08	14.3	0.021	0.020	.172	.075
242	0.62	43	41.15	16.20	14.3	0.021	0.020	.200	.076
243	0.62	43	43.80	16.28	14.3	0.021	0.020	.213	.077
244	0.62	43	47.03	16.10	14.3	0.021	0.020	.229	.075
245	0	15	43.02	14.67	5.0	0	0.033	.355	.100
246	0	15	26.14	14.65	5.0	0	0.033	.216	.110
247	0	15	44.83	14.50	5.0	0	0.033	.370	.108
248	0	15	57.67	14.78	5.0	0	0.033	.475	.112
249	0	15	16.12	14.28	5.0	0	0.033	.133	.106
250	2.6	15	28.79	13.48	5.0	0.087	0.033	.237	
251	2.6	15	38.39	12.98	5.0	0.087	0.033	.316	
252	2.6	15	50.02	12.88	5.0	0.087	0.033	.412	
253	2.6	15	58.00	13.00	5.0	0.087	0.033	.478	
254	2.6	15	31.22	13.13	5.0	0.087	0.033	.257	
255	2.6	15	42.13	13.58	5.0	0.087	0.033	.347	
256	2.6	15	48.16	13.25	5.0	0.087	0.033	.397	
257	0	15	20.70	12.58	5.0	0	0.070	.148	.204
258	0	15	34.74	12.90	5.0	0	0.070	.248	.205
259	0	15	41.72	12.38	5.0	0	0.070	.298	.191
260	0	15	28.46	12.80	5.0	0	0.070	.203	.202
261	0	15	17.87	12.50	5.0	0	0.070	.128	.194
262	0	15	45.11	12.85	5.0	0	0.070	.322	.203
263	0	15	53.48	12.95	5.0	0	0.070	.382	.206

TABLE 2

## AVERAGE VALUES OF k

$\frac{\Delta}{\Lambda}$	$D_{50}/\Delta$			
	0.00	0.021	0.040	0.087
.02	.079	.077	.066	.058
.033	.107	-	.098	.088
.05	.143	-	.141	.137
.07	.199	-	-	-

TABLE 3

## BED-LOAD DISCHARGE COEFFICIENT K

$\frac{\Delta}{\Lambda}$	$D_{50}/\Delta$			
	0.00	0.021	0.040	0.087
.02	1.68	1.69	1.74	1.77
.033	1.57	-	1.61	1.65
.05	1.43	-	1.44	1.45
.07	1.20	-	-	-

TABLE 4 COMPUTED BED LOAD USING  $K = K \left[ \Delta/\Lambda, D_{50}/\Delta \right]$

Run No.	$\epsilon$ m	$U_w$ $10^4$ m/s	$G_{sm}$ Kg/s/m	$\frac{\Delta}{\Lambda}$	$\frac{D_{50}}{\Delta}$	K	$G_{sc}$ Kg/s/m	E %
1	.0201	6.02	.0166	.062	.018	1.30	.0143	-14.0
3	.0191	6.25	.0161	.049	.020	1.45	.0157	- 2.5
4	.0164	5.37	.0089	.052	.020	1.42	.113	27.5
5	.0175	6.52	.0177	.044	.025	1.51	.0156	-11.5
6	.0185	10.87	.0336	.041	.024	1.54	.0281	-16.4
7	.0162	4.20	.0107	.039	.023	1.56	.0096	- 9.9
8	.0207	7.33	.0171	.045	.024	1.50	.0206	20.8
13	.0147	6.75	.0128	.050	.026	1.45	.0131	2.0
14	.0179	7.79	.0153	.048	.026	1.47	.0186	21.5
15	.0179	9.09	.0174	.054	.021	1.40	.0207	18.8

TABLE 5 EFFECT OF BED-LOAD COEFFICIENT

Run No.	K=1.32		$K = K \left[ \Delta/\Lambda, D_{50}/\Delta \right]$		$G_{sm}$ Kg/s/m
	$G_{sc}$ Kg/s/m	%E	$G_{sc}$ Kg/s/m	%E	
1	.0145	-12.7	.0143	-14.0	.0166
3	.0143	-11.2	.0157	- 2.5	.0161
4	.0106	19.1	.113	27.5	.0089
5	.0137	-22.6	.0156	-11.7	.0177
6	.0237	-29.5	.0281	-16.4	.0336
7	.0083	-22.4	.0096	- 9.9	.0107
8	.0182	6.4	.0206	20.8	.0171
13	.0119	- 7.0	.0131	2.0	.0128
14	.0167	9.2	.0186	21.5	.0153
15	.0195	12.1	.0207	+18.8	.0174
E		- 5.9		+3.6	



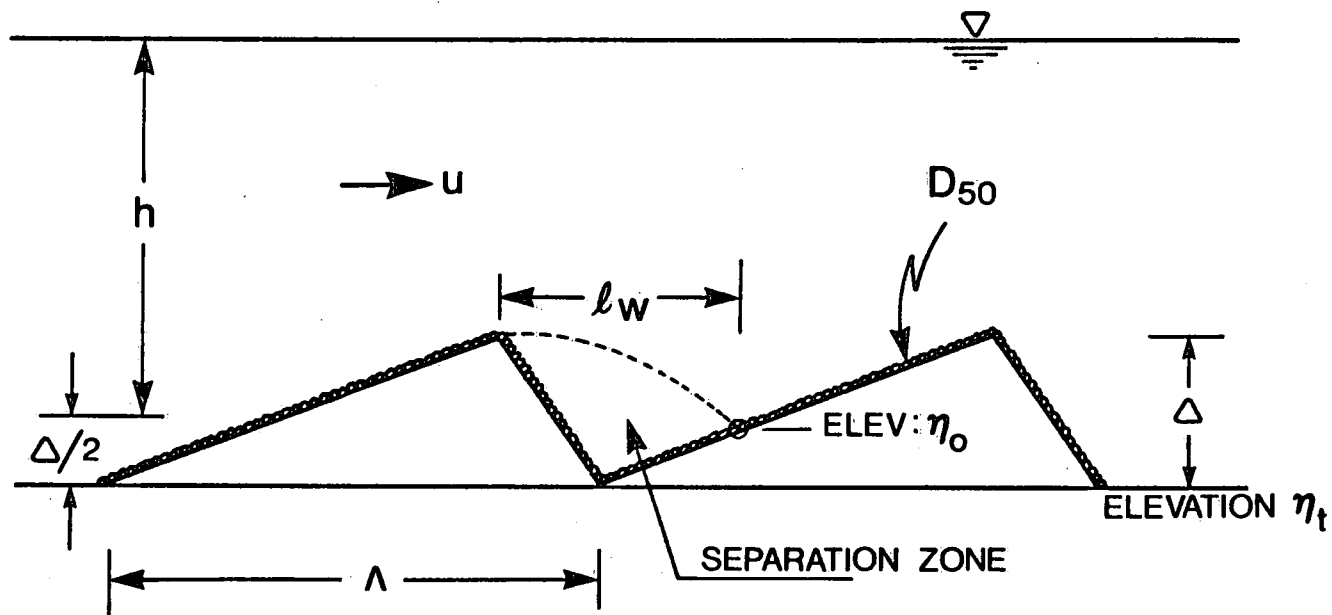


FIGURE 1. DEFINITION SKETCH

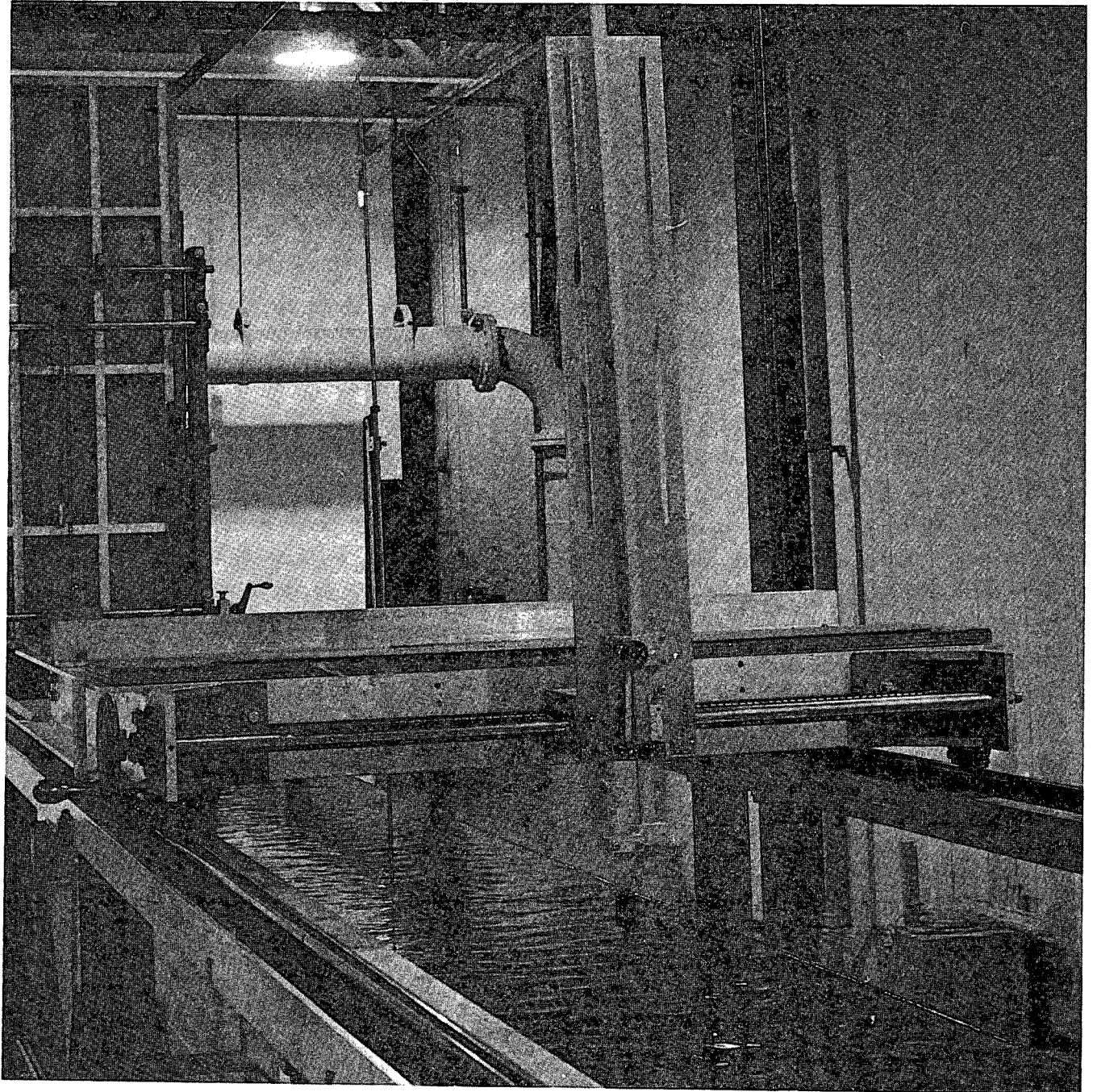


FIGURE 2. DYE INJECTION APPARATUS

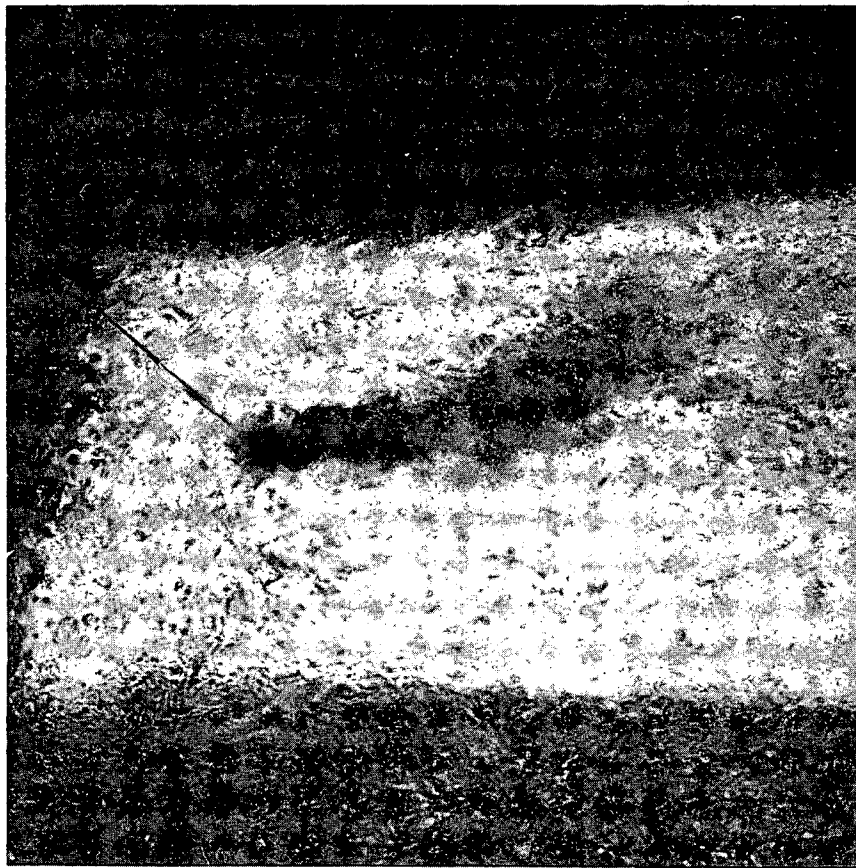


FIGURE 3a. DYE DOWNSTREAM OF RE-ATTACHMENT POINT

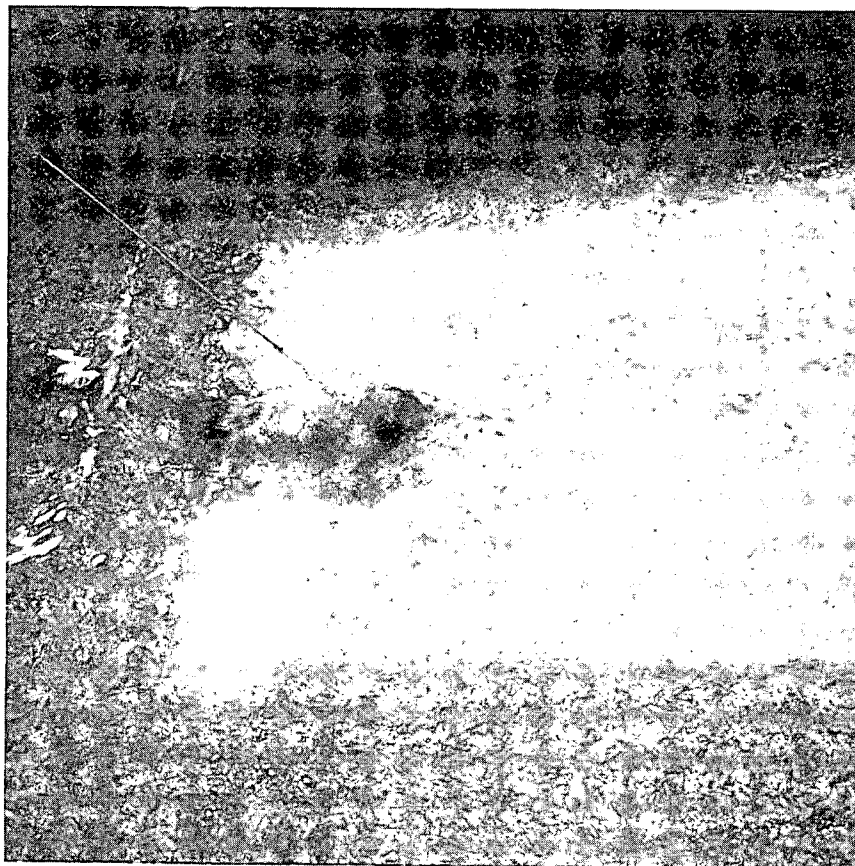


FIGURE 3b. DYE UPSTREAM OF RE-ATTACHMENT POINT

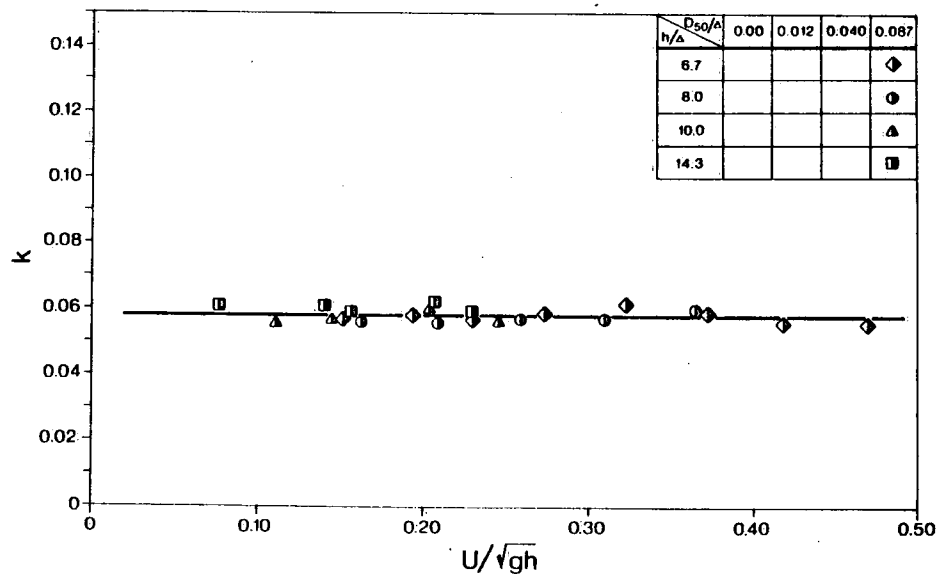
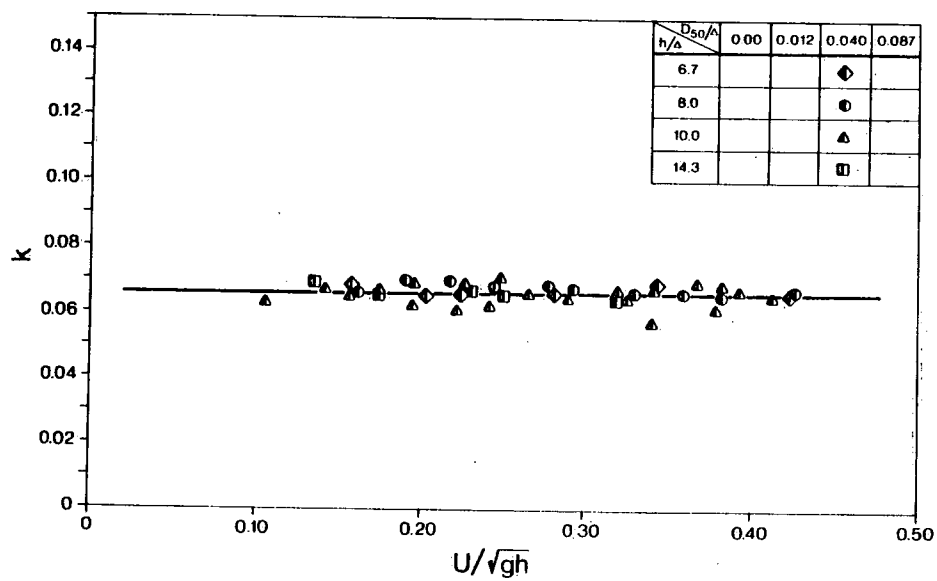
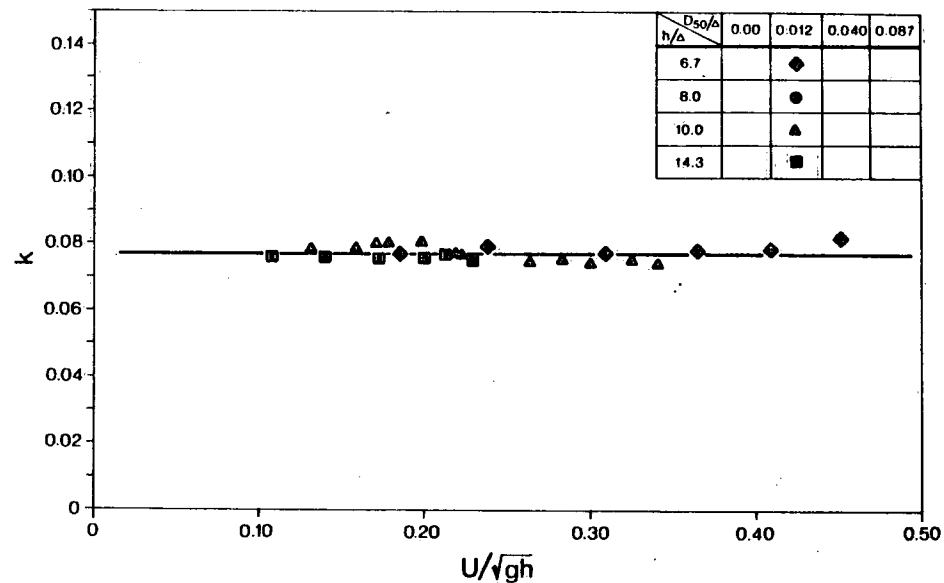
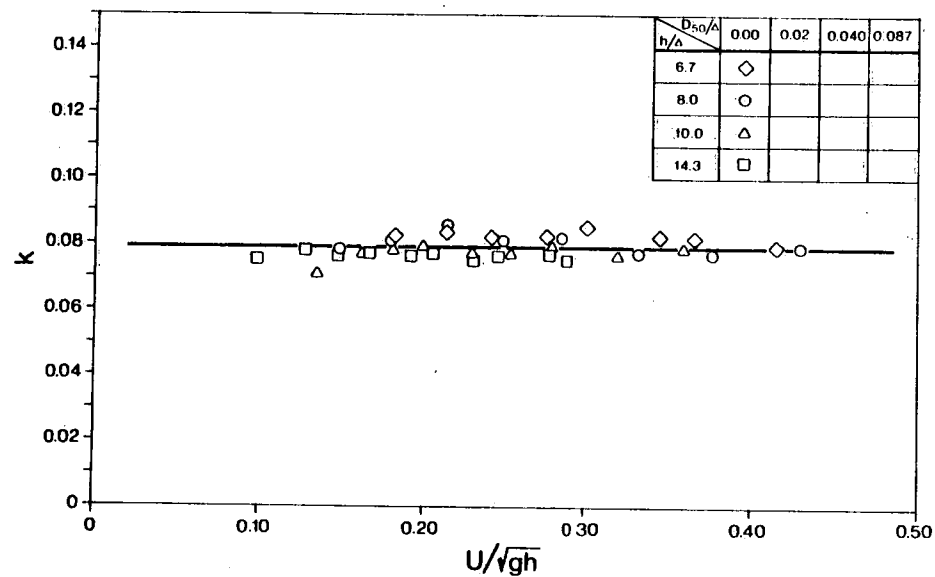


FIGURE 4. VARIATION OF  $k$  WITH FROUDE No. WHEN  $\Delta/\lambda = 0.02$

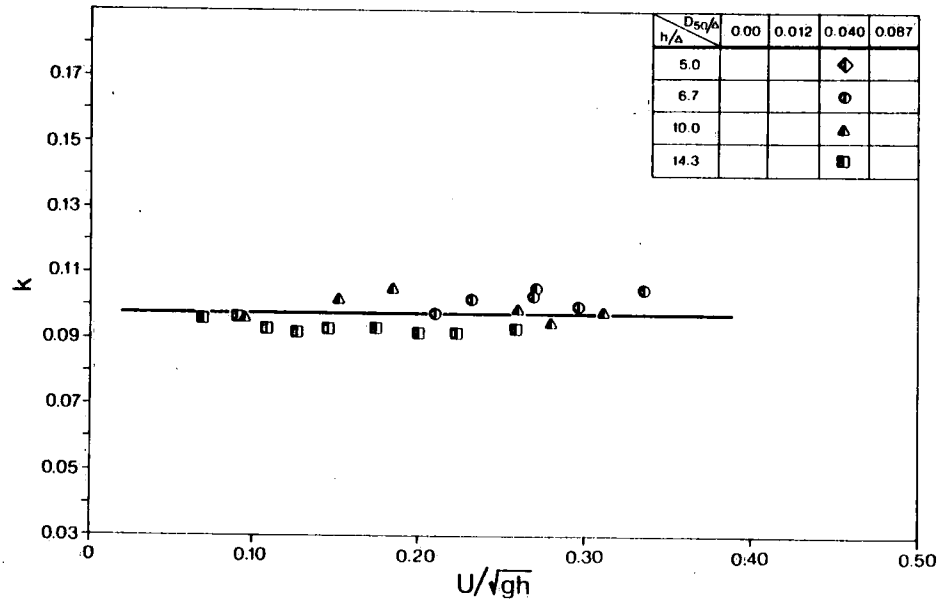
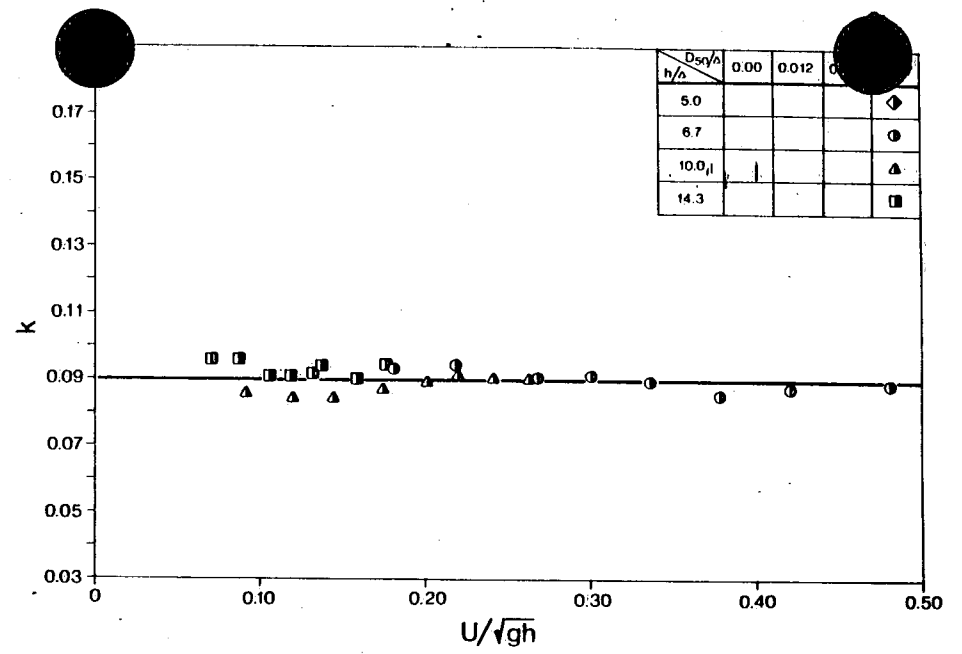
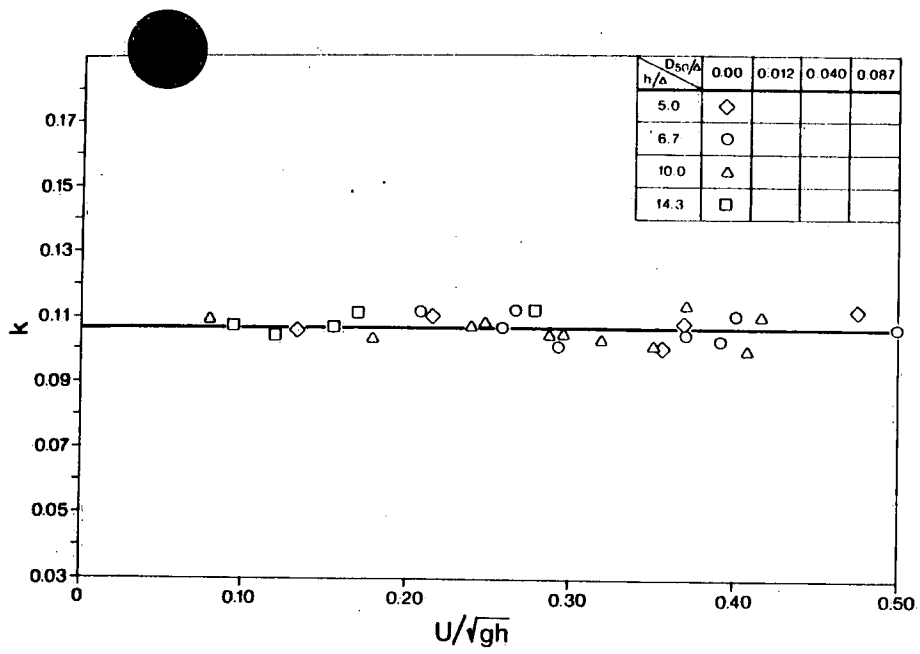


FIGURE 5. VARIATION OF  $k$  WITH FROUDE No. WHEN  $\Delta/\lambda=0.033$

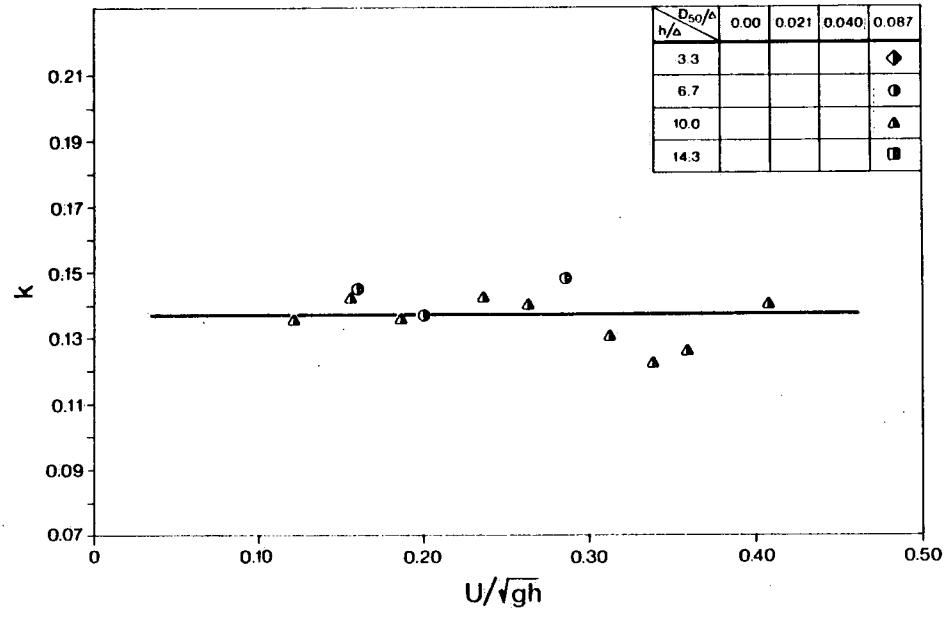
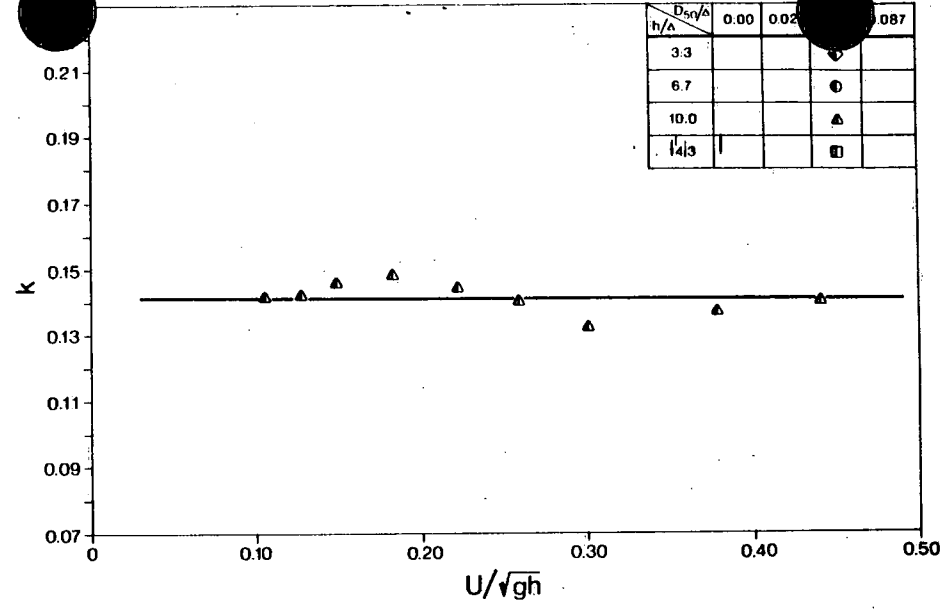
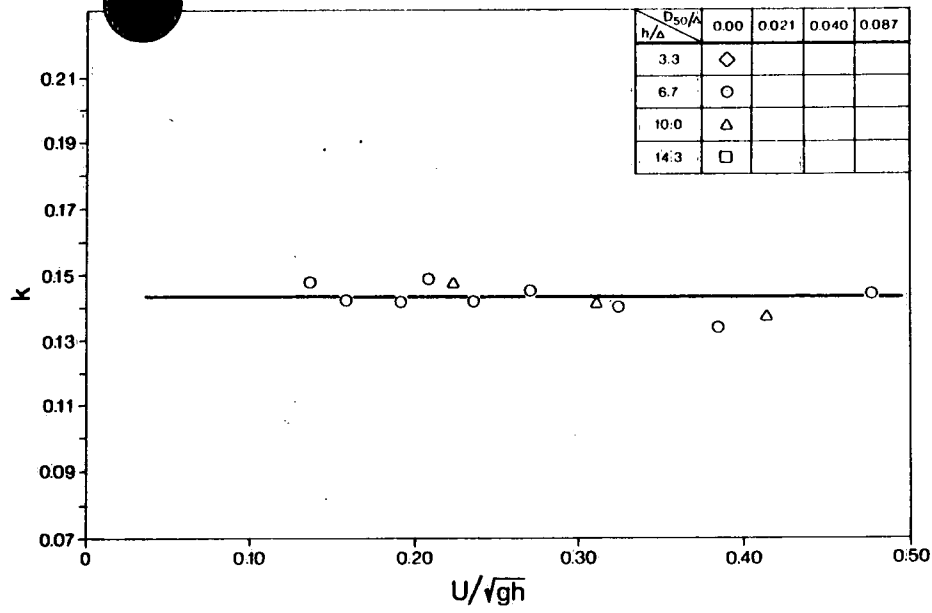


FIGURE 6. VARIATION OF  $k$  WITH FROUDE  $No.$  WHEN  $\Delta/\lambda = 0.05$

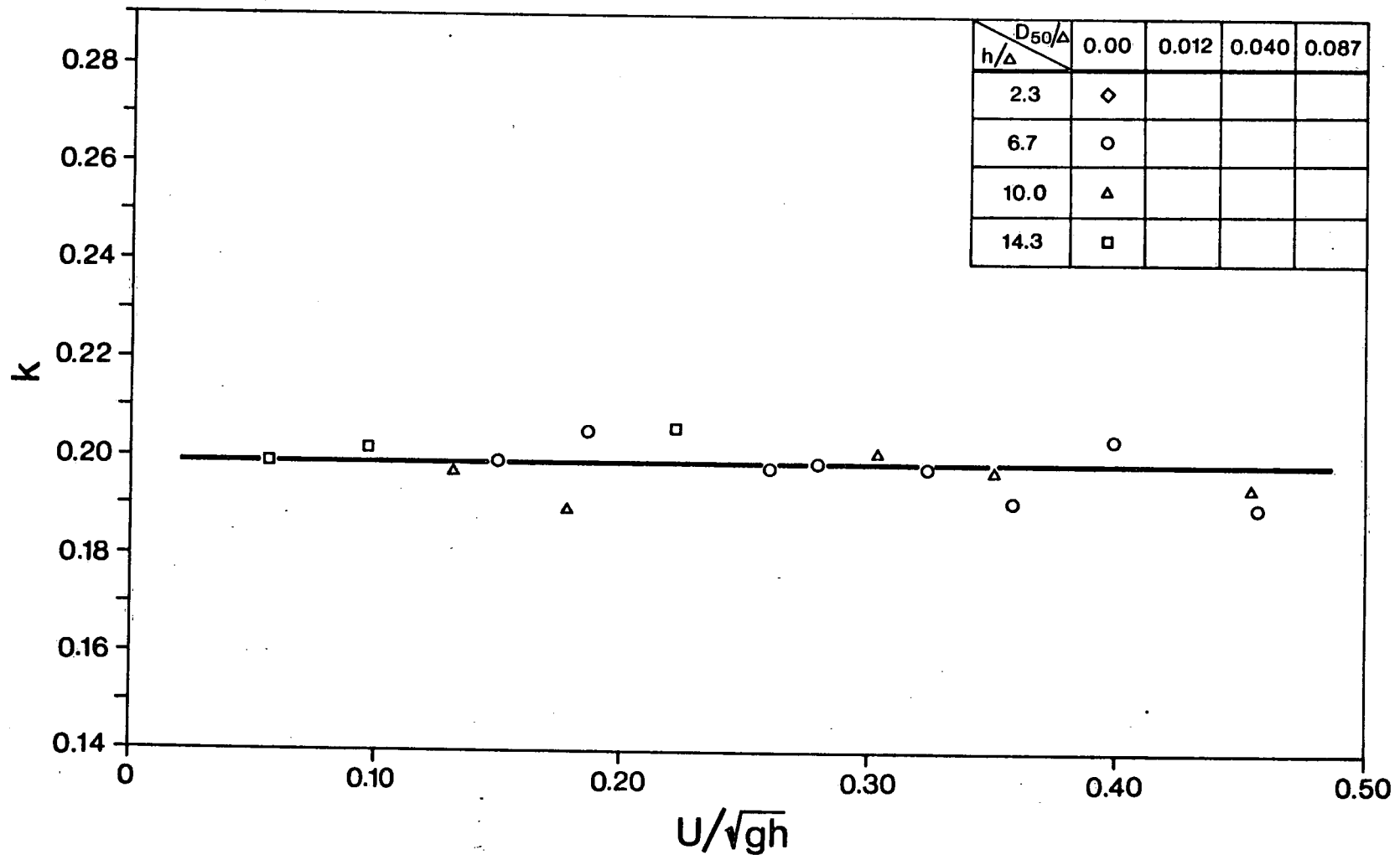


FIGURE 7. VARIATION OF  $k$  WITH FROUDE No. WHEN  $\Delta/\lambda = 0.07$

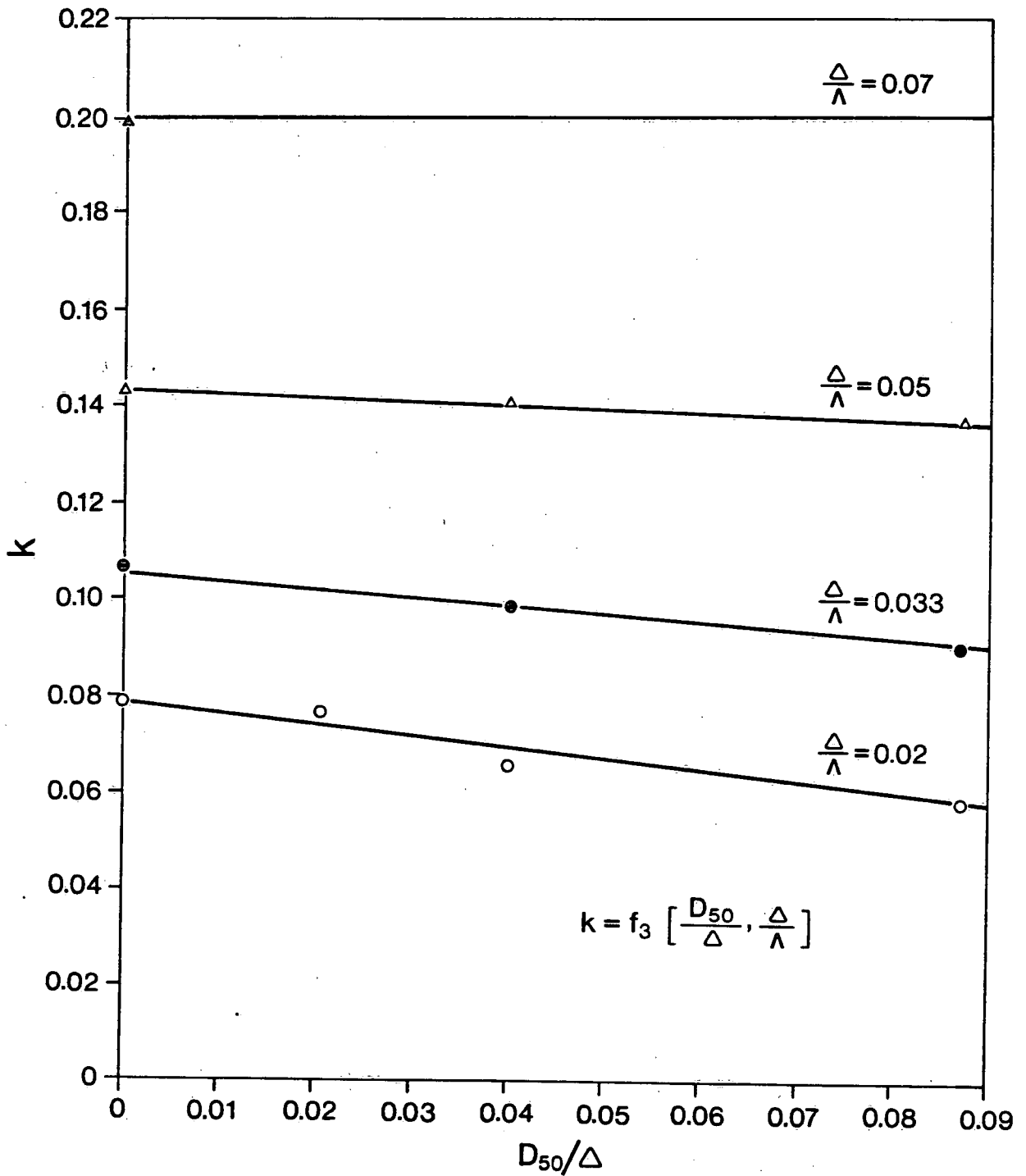


FIGURE 8. EFFECT OF SAND SIZE ON  $k$



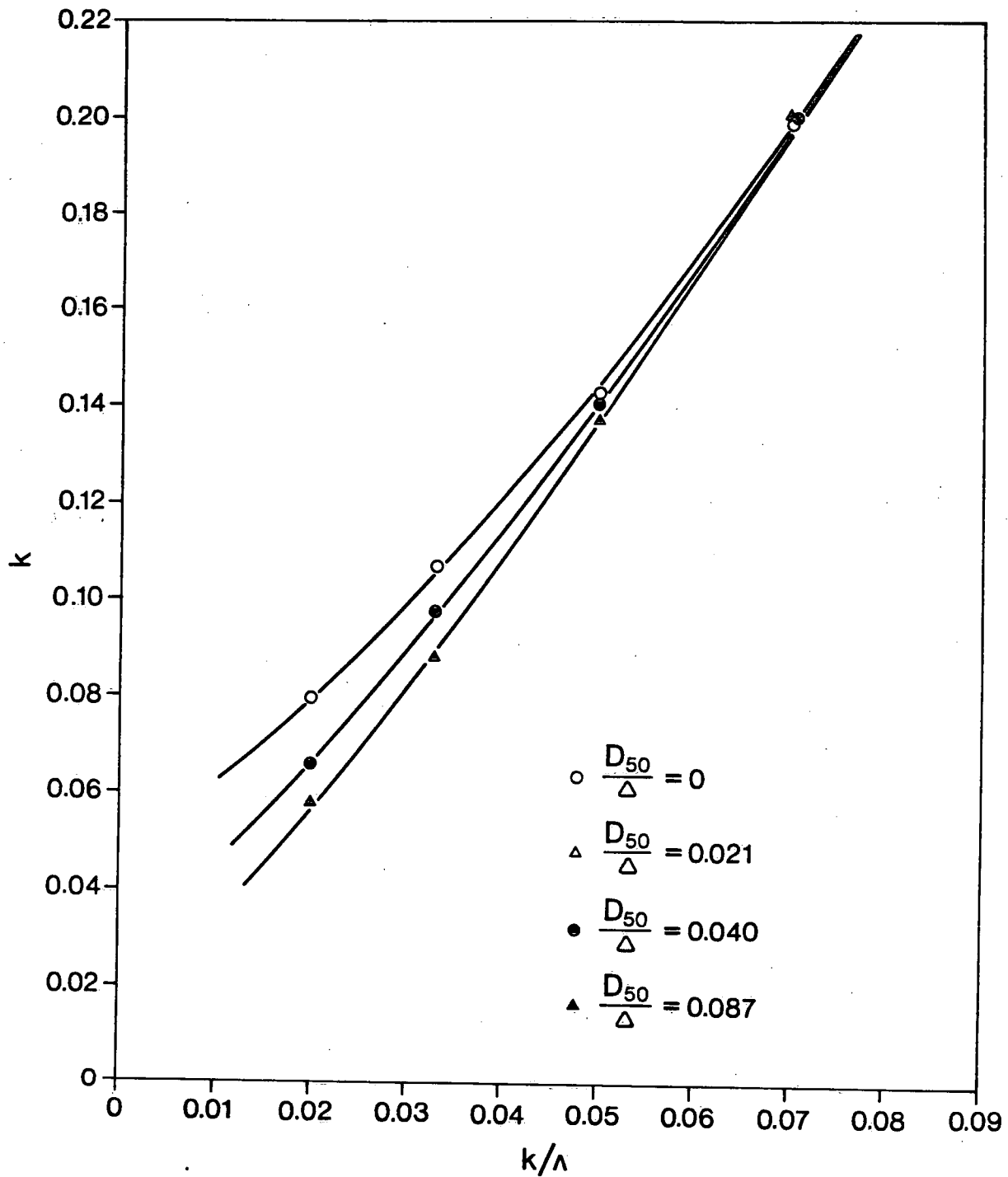


FIGURE 9. VARIATION OF  $k$  WITH DUNE STEEPNESS

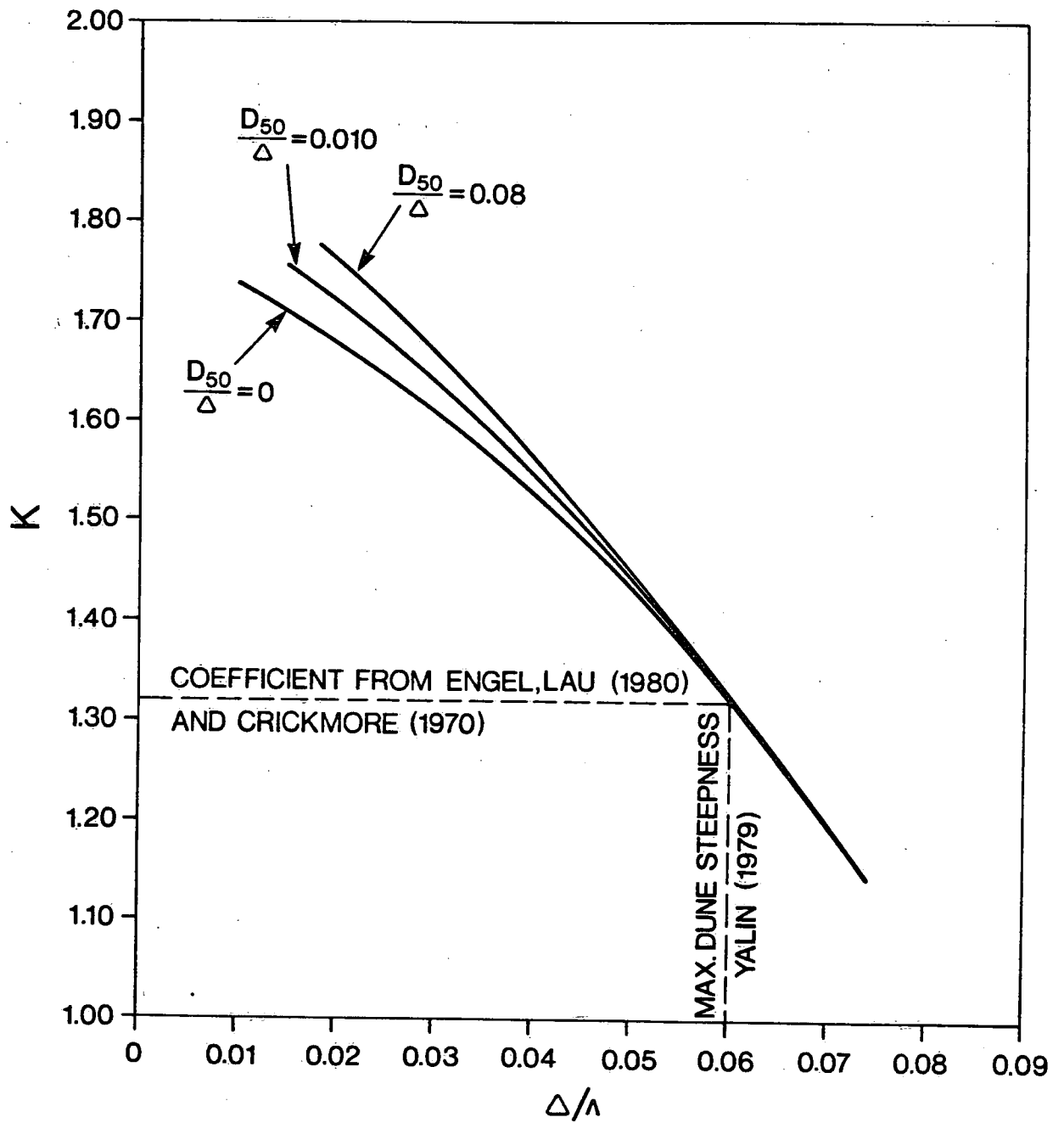


FIGURE 10. BEDLOAD DISCHARGE COEFFICIENT

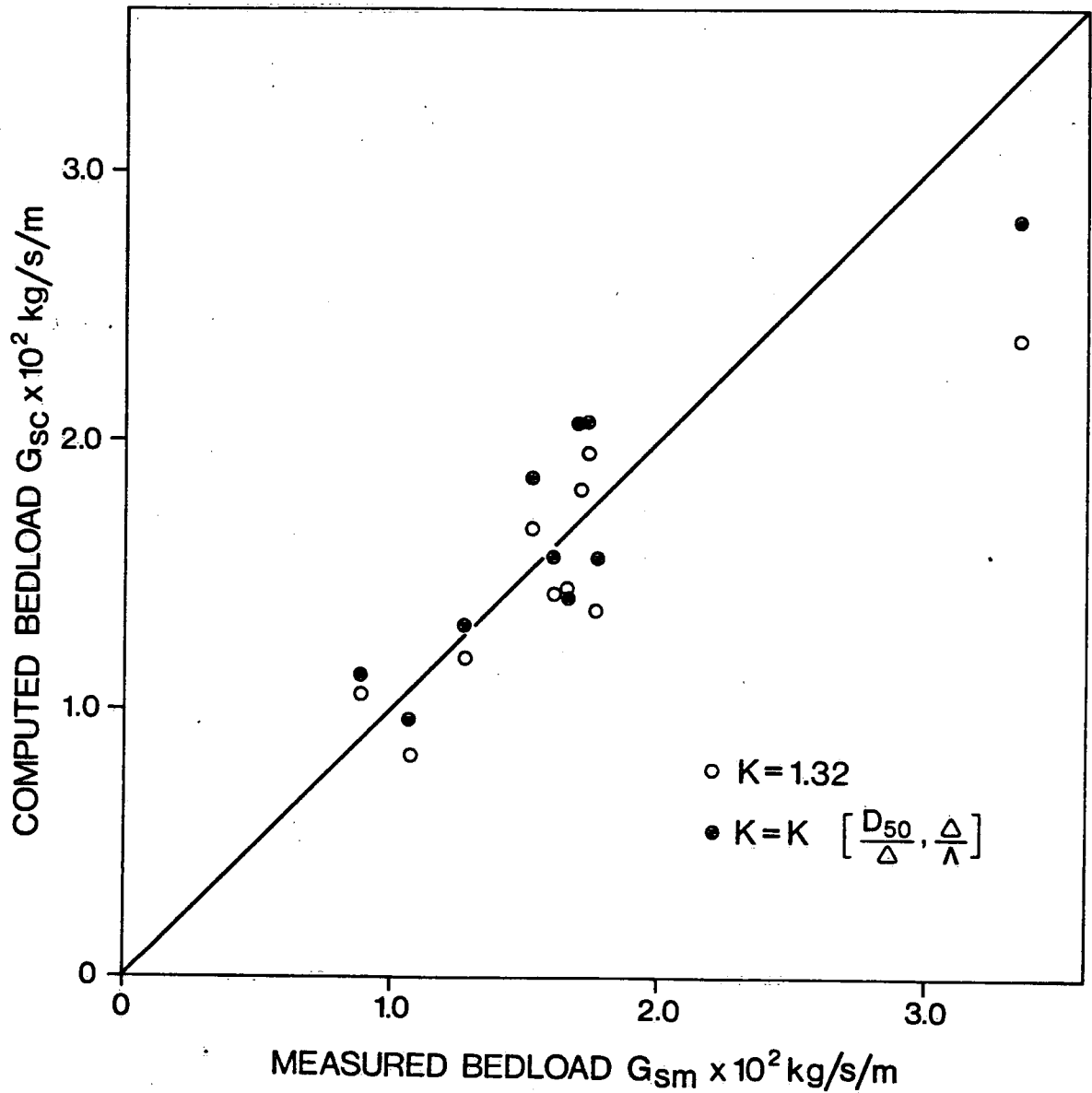


FIGURE 11. EFFECT OF BEDLOAD COEFFICIENT

15735

ENVIRONMENT CANADA LIBRARY, BURLINGTON



3 9055 1016 7341 5